Materials Transactions, Vol. 55, No. 8 (2014) pp. 1219 to 1225
Special Issue on Thermoelectric Conversion Materials VIII

Simulation of a Thermoelectric Module Having Parallelogram Elements

Xiangning Meng[1,2,*], Takeyuki Fujisaka[1], Keita O. Ito[1] and Ryosuke O. Suzuki[1,3]

[1]*Faculty of Engineering, Hokkaido University, Sapporo 060-8628, Japan*
[2]*School of Materials and Metallurgy, Northeastern University, Shenyang 110819, China*
[3]*Japan Science and Technology Agency (JST), Tokyo 102-8666, Japan*

A thermoelectric (TE) module with two different thermal sources for power generation is studied in this work. Here, a conventional Π-type module is tilted in the shape of a parallelogram. A numerical analysis is conducted by using the finite volume method to examine three-dimensional (3-d) flows of heat and electric charge. The module configuration and the shape of the elements determine the distribution of temperature and current density inside the TE module. Further, the shortest path is chosen preferentially as the path of the current, depending on the geometry of the TE elements. Although the distribution of current density depends greatly on the module configuration, the TE output power is not affected by the parallel and symmetrical configurations in the two equivalent modules. Thus, the conventional TE module with Π-type elements is the most favorable, and maximum performance is obtained for a tilting angle of 90° because of the lowest internal electric resistance.
[doi:10.2320/matertrans.E-M2014822]

(Received September 30, 2013; Accepted April 14, 2014; Published June 6, 2014)

Keywords: *thermoelectric generation, Π-type module, heat transfer, current density, finite element analysis*

1. Introduction

The heat at a junction of two different materials can be directly converted into electricity by using a thermoelectric (TE) generation (TEG) system, which is based on the Seebeck effect. This method has many advantages. It can use inexhaustible resources and low-grade energy, such as renewable solar heat and unrecovered waste heat, and it is noiseless, pollution free, and operational even in isolated places. Additionally, chemical reactions or mechanical moving parts are not needed in the TEG. Many studies focused on the improvement of the inherent properties of thermoelectric materials.[1–3] However, the low-conversion efficiency is a distinct disadvantage.[4,5] Other factors for maximizing efficiency are the optimal design of the TEG and the improvement of the properties of TE materials.[6] Optimizing the TEG design is critical for obtaining maximum performance because the output power of the TEG system is significantly enhanced by thermally and electrically combining the TE elements in series.[7] Optimization of the number of p-n pairs, the shape of the multi-stage TE panels, and the module geometry were studied to obtain the best performance.[8–10] As a fundamental cell, the Π-type TE module is one of the most popular configurations. The schematic of a large-scale TE system with the conventional Π-type structure is shown in Fig. 1(a). In this system, the current flows through the Π-type channel to generate power. The preferential flow of current in a certain path in a 3-d body is proposed.[11] This current path is chosen spontaneously, reflecting the shape of the TE element, and is governed by the detailed configuration and dimensions of the TE system. This non-uniform current flow may provide a new concept for better efficiency.

Recently, a tubular TE device consisting of tilted multi-layer was proposed.[12,13] Tight connections of the slanted elements were essential to effectively use the thermal energy of fluid. A good design of heat conduction and electric properties could successfully produce a high TE power. The crystalline orientation of the TE material might be one of the reasons for the high TE power. However, the design details of the module have not been analyzed. Although it may have a decisive effect on the electric current flow, the arrangement of the TE elements as a parallelogram has not yet been examined. Moreover, the flow of electric charge in the 3-d cylindrical portion has not been mathematically analyzed. Here, we assumed the isotropic properties of materials to investigate the macro-scopic phenomena and TE performance, and temporarily we neglected the crystalline anisotropy. If some differences exist in the experiments, it is due to the preferred orientation in which this paper has not been handled. The consideration of the crystalline orientation of materials requires a recoding in the host program FLUENT for numerical simulation. It also needs the successive confirmation of healthy working. Under a limitation in the currently available calculating tools, the isotropic properties in the materials are assumed, and we desired that the resultantly numerical evaluation will express some insights for construction of TE elements.

The purpose of this study is to investigate the effect of tilting the TE elements by numerical analysis using a simplified module as an example. The tilting angle (θ) is defined as shown in Fig. 1(b). The conventional Π-type is a special case when the tilting angle is 90°. This work emphasizes the basic phenomenon of a TE module with tilted elements under a constant temperature difference, as well as analyzes the effect of tilting angle of the TE element on the performance of the TE module.

2. Modeling

2.1 Finite element entity model

This study will analyze a TE module with the p- and n-type elements connected in series such as a Π-type module. Finite element analysis is applied to examine the 3-d effects. For simplicity, however, configuration data, except the tilting angle (θ), of the TE module are fixed and listed in Table 1.

*Corresponding author, E-mail: mengxn@eng.hokudai.ac.jp

Table 1 Configuration data of TE module.

p-n pairs	Elements (p-type and n-type)			Electrodes		Insulators	
	Area (mm^2)	Leg length (mm)	Width (mm)	Thickness (mm)	Width (mm)	Thickness (mm)	Width (mm)
18	1.0	1.0	1.0	0.1	1.0	0.5	1.0

Table 2 Thermal and electric properties of materials.[14)]

	Seebeck coefficient ($\mu V \cdot K^{-1}$)	Thermal conductivity ($W \cdot m^{-1} \cdot K^{-1}$)	Electric resistivity ($\mu\Omega \cdot m$)	Figure-of-Merit (−)
Bi_2Te_3 (p-type)	190 (300–500 K)	2.06	5.5	>0.9 (300–600 K)
Bi_2Te_3 (n-type)	−210 (300–500 K)	2.02	10.0	>0.9 (300–600 K)
Cu (electrode)	1.83 (300 K)	398	0.0155	
Al_2O_3 (insulator)		36	0	

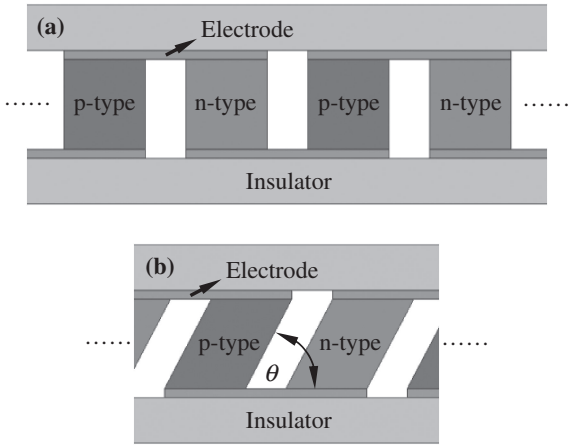

Fig. 1 Π-type TE modules of (a) conventional and (b) with tilting angle θ.

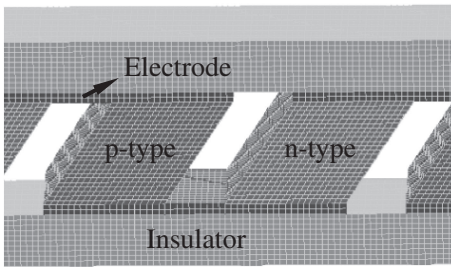

Fig. 2 Meshed entity model for finite element analysis.

All the TE elements were tilted at the same θ. An entity model of the TE module is three-dimensionally meshed, and a part of the TE junction of this model is shown in Fig. 2. The properties of the materials[14)] for finite element simulations of the TE phenomenon are listed in Table 2. These properties are considered as temperature-independent in order to clarify the fundamental regularities of TE process. The following assumptions were made while designing the models: (1) the entire TE system is adiabatic; (2) tight bonding is achieved among all the parts; and (3) the properties of the materials are temperature independent and isotropic.

2.2 Analytical model

Macroscopically, the heat balance of the TE system can be illustrated as shown in Fig. 3. This heat balance can be expressed as eqs. (1) and (2). Then, the theoretical output power (P) can be deduced as eq. (3).

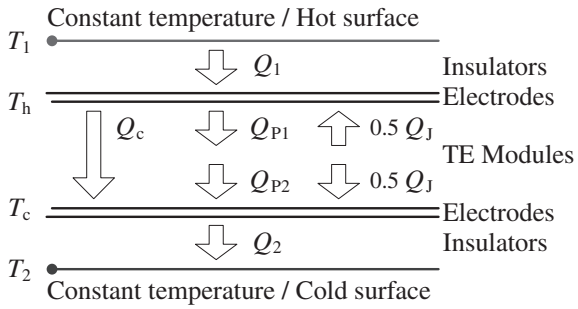

Fig. 3 Schematic representation of heat balance of TE system.

$$Q_1 = Q_c + Q_{P1} - 0.5Q_J \quad (1)$$

$$Q_c + Q_{P2} + 0.5Q_J = Q_2 \quad (2)$$

$$P = Q_{P1} - Q_{P2} - Q_J \quad (3)$$

Here, Q_1 and Q_2 denote the heat conducted through the insulator and electrode layers, respectively, and Q_{P1} and Q_{P2} denote the Peltier heat that depends on the temperature and current. These heats appear at the interfaces between the electrodes and the TE modules, and T_h and T_c are the temperatures at these interfaces. Moreover, T_1 and T_2 are the temperatures of the hot and cold surfaces of the electrodes, respectively. Additionally, Q_J and Q_c are the Joule heat following the Joule law and the total heat conducted through all the TE modules, respectively, and P is the output power of the TEG.

The internal heat transfer and electric charge transportation are analyzed using the thermal diffusion and charge transportation equations in addition to the TE phenomenon. The differential equations for the heat conduction at each finite element volume are solved on the basis of energy conservation. The heat and electric charge balances in a control volume are shown in Fig. 4, where q and J denote the heat and current density, respectively.

The heat-conduction equation under steady-state conditions is given by eq. (4) as follows.

$$\nabla \cdot (\lambda \Delta T) + \rho |\boldsymbol{J}|^2 - T\boldsymbol{J} \cdot \nabla S = 0 \quad (4)$$

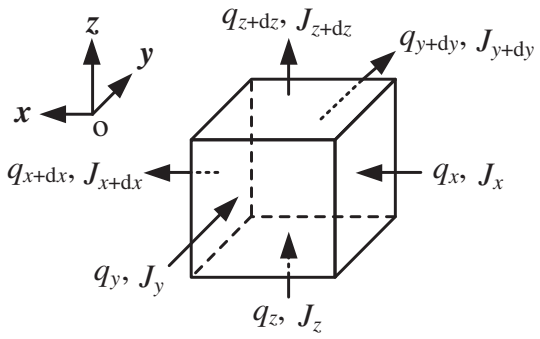

Fig. 4 Heat and electric charge balances in finite element volume.

Here, the three terms represent the heat conduction, the Joule heat generated by the current along the finite element volume, and the heating or cooling generated by the Thomson effect, respectively. Further, λ, ρ, and S denote the thermal conductivity, specific electric resistivity, and relative Seebeck coefficient, respectively, and $\boldsymbol{J}$ is the current density determined by the electric potential and temperature using eq. (5). Further, Ohm's law is expressed as

$$\rho \boldsymbol{J} = -\nabla V - S\nabla T \tag{5}$$

where the voltage due to $\rho \boldsymbol{J}$ is expressed by the change of electric potential (∇V) and the voltage generated from the Seebeck effect ($S\nabla T$). The differential equation, i.e., eq. (6), is derived from eq. (5) by applying charge conservation under steady-state conditions.

$$\nabla \cdot \left(-\frac{1}{\rho} \nabla V \right) = \nabla \cdot \left(-\frac{s}{\rho} \nabla V \right) \tag{6}$$

The temperature and electric potential distributions are obtained by solving the simultaneous differential equations. Equations (4) and (6) are solved numerically with the finite volume method based on the commercial software, FLUENT. The contribution of the TE phenomenon was originally coded by home-made C program,[15] and then combined with the conventional functions of FLUENT, because the optional function in the commercial software did not contain the calculations for TE phenomenon, such as current density.

3. Results and Discussion

3.1 Temperature and current density profiles

The heat flux from the hot source to the cold source was calculated to be nearly constant because the thermal conditions were fixed at the external boundaries of the TE module and a potential difference was generated in the entire module because of the TE phenomena. The temperature and current density in a single pair of TE elements having a tilting angle of 45° are shown in Fig. 5. The temperature changes steadily from the hot to cold sources in the TE module conductors. This change is identical in the two types of TE materials having different properties because the thermal conditions are assumed to be fixed and the elements are of the same shape. A gradient in the temperature profile is typical because of the shape of the tilted elements. The angle between the tilted elements and the direction of thermal conduction form the hierarchical isothermal surface. The isothermal profiles in the central region are parallel reflecting the constant temperature gradient, and those close to the hot and cold sources are not parallel, as shown in Fig. 5(a). The current density is also significantly affected by the shape of the tilted elements, and a clear asymmetric distribution of current density appears particularly at the electrode plate. This asymmetry in the electrode is particularly serious at positions close to the TE elements when a thin electrode plate is used as a narrow channel for the flow of electric charge. Moreover, high-density regions are formed and cover relatively large areas in the electrodes, as indicated by black arrows in Fig. 5(b). Additionally, other high-density regions containing the maximum density points cover relatively smaller areas, as indicated by red arrows.

3.2 Comparison of equivalent modules

Here, the performance of the two TE modules having equivalent dimensions, as shown in Fig. 6, is compared to analyze the effect of the tilted TE element configuration. Both the models contain TE electrodes and insulators of the same size and the same volume of TE elements. The only difference between the two models is that the p- and n-type elements are welded to the electrodes at the complementary angles of $\theta = 45°$ and 135°. Interestingly, the TE performance of the two TE modules is almost identical, as listed in Table 3, although the values of the module having parallel elements ($\theta = 45°$) are slightly greater than that having symmetrical elements ($\theta = 135°$).

Nevertheless, the distribution of temperature and current density inside the TE elements varies with the module configuration, as shown in Fig. 6. The temperature profiles present a characteristic gradient based on the element shape, as shown in Figs. 6(a)-1 and 6(b)-1. However, an area at a higher temperature does not correspond to a higher current density. The current density is distributed almost homogenously inside the TE elements, as shown by the color progression, whereas the details in the distribution of current density are affected by the module configuration. The low-density regions in the n-type element are located far away from the high-density region, which is at the contact position between the electrode and the element, in the parallel configuration ($\theta = 45°$). However, the low-density regions in the n-type element are close to the high-density region at the contact position in the symmetrical configuration ($\theta = 135°$). Hence, the low-density regions are located at both the terminals of the longer diagonal, whereas the shorter diagonal connects the two terminal regions with the higher current density region indicating that the current flows preferentially through the shortest path.

The contours of current density are shown in Figs. 6(a)-3 and 6(b)-3 and look like two opposite views of an "open book" fixed at two electrodes. Here, most of the electric charge flows along the shortest path, which we define as the mainstream of the current. The rest of the charge moves along the longest path, which can be defined as the sidestream of the current. The main- and sidestreams of the current meet at the center of the element thus forming a homogenous high-density region. This concept is illustrated

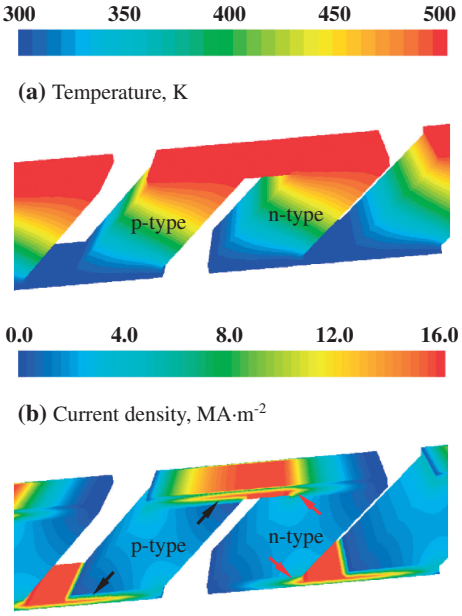

Fig. 5 Distributions of temperature (a) and current density (b) in a pair of TE elements ($\theta = 45°$).

Table 3 TE performances of two TE modules.

Styles	Voltage (W)	Current (A)	Output power (W)
parallel	0.456	1.934	0.881
symmetrical	0.455	1.930	0.878

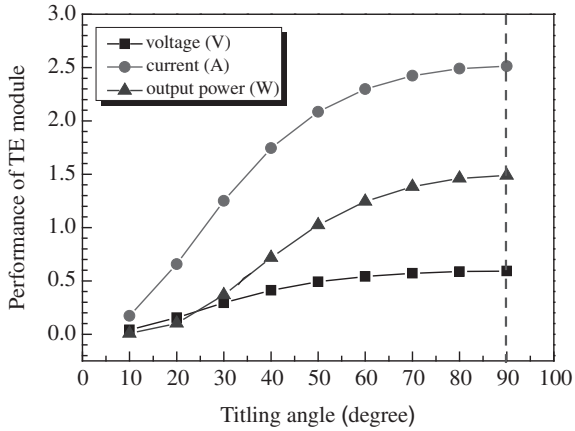

Fig. 7 Performance of TE module as a function of tilting angle.

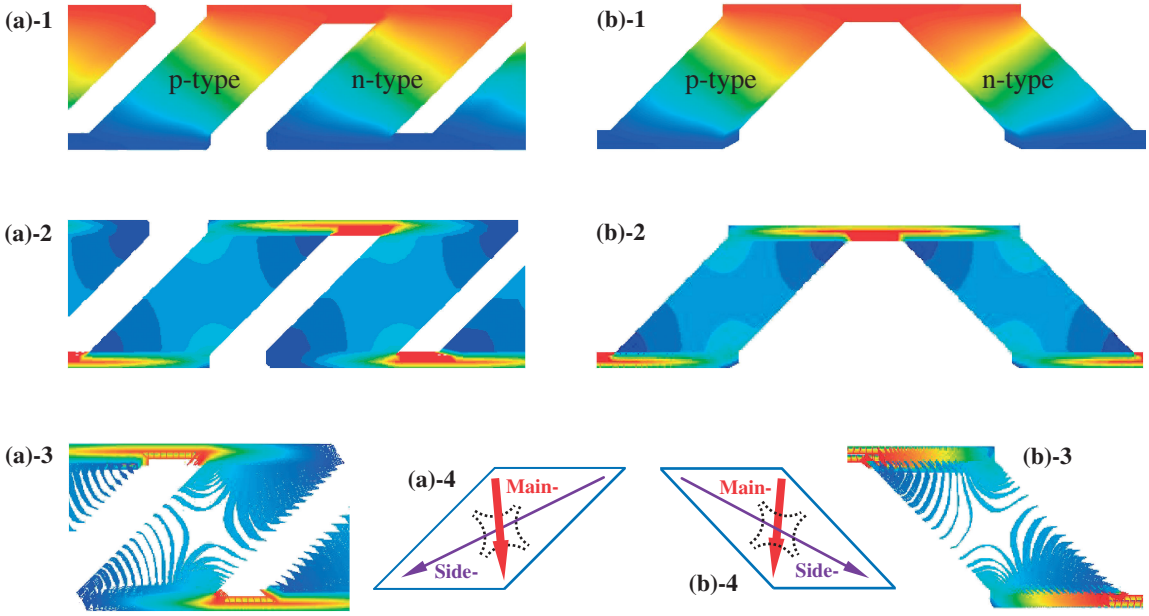

Fig. 6 Temperature and current density inside TE elements of (a) parallel and (b) symmetrical. 1: temperature distribution, 2: distribution of current density, 3: contour plots of current density.

with the simplified diagrams shown in Figs. 6(a)-4 and 6(b)-4.

3.3 Tilting-angle dependency

The difference in the performance of the two TE modules ($\theta = 45°$ and 135°) is small. However, the tilting angle has a significant impact on their TE performance, as shown in Fig. 7, where we assume that the basal area and height of the elements are fixed, and the volume of the TE materials remains constant. The internal electric resistance of the TE module is dependent on the geometry of the elements, i.e., the tilting angles. A lower resistance is induced at a larger tilting angle (θ) as given by eq. (7).

$$R_{\mathrm{i}} = \sum_{k=1}^{m} \left(\rho_{\mathrm{p}}^{k} \frac{L_{\mathrm{p}}^{k}}{A_{\mathrm{p}}^{k}} + \rho_{\mathrm{n}}^{k} \frac{L_{\mathrm{n}}^{k}}{A_{\mathrm{n}}^{k}} \right) \tag{7}$$

Here, R_{i} and m denote the internal electric resistance of the TE module and the number of p-n pairs, respectively, and L and A denote the length and cross-sectional area of the TE elements, respectively. Further, subscripts p and n represent p- and n-type materials, respectively.

Both the voltage and current in the TE module increase because the electromotive force (EMF) in the electric circuit is constant for fixed steady-state thermal conditions and Seebeck coefficients. The tilting angle has a small effect on the voltage but has a more significant impact on the current,

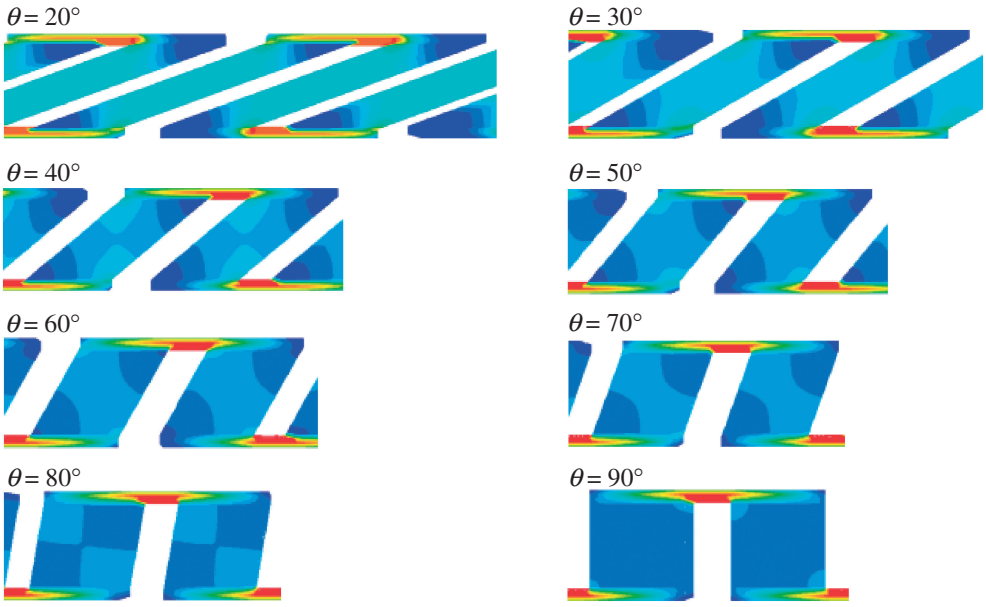

Fig. 8 Distribution of current density at various tilting angles.

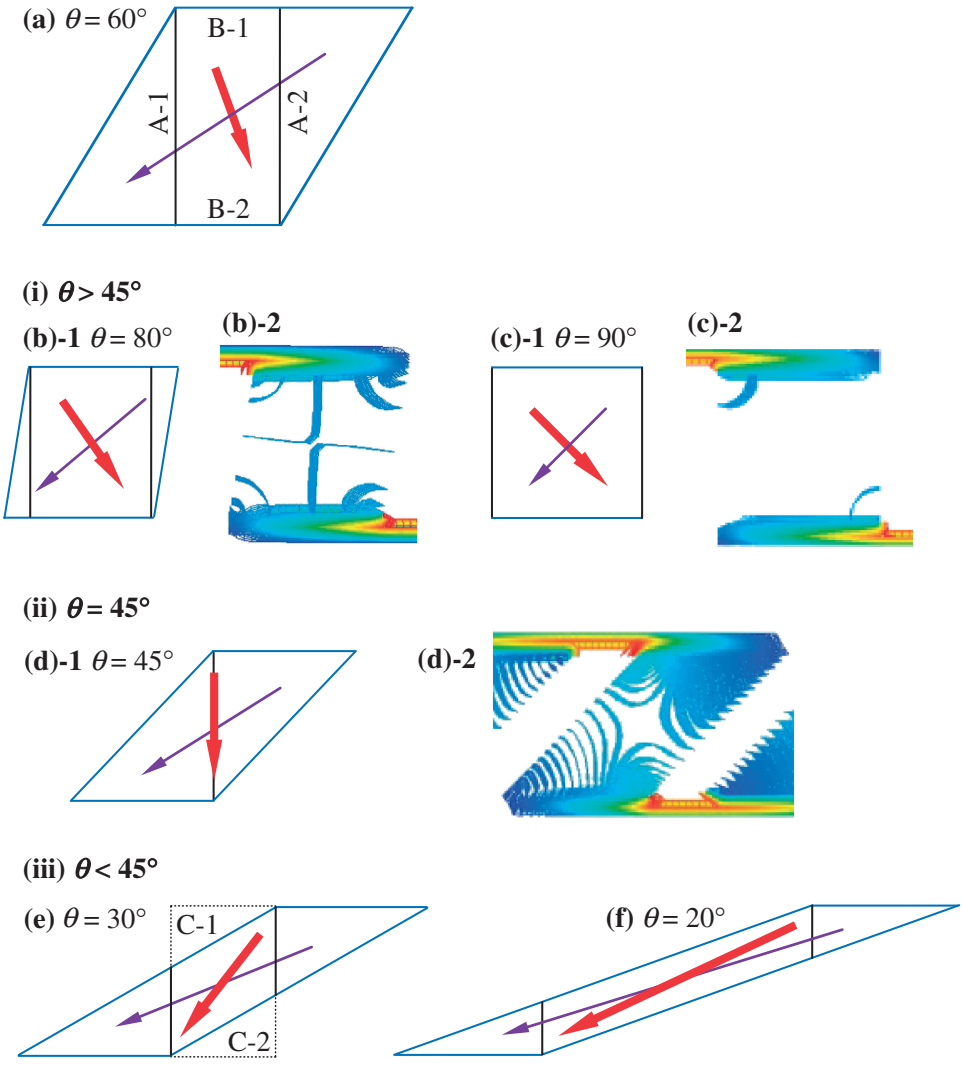

Fig. 9 Analysis for effect of tilting angle on current density distribution.

as shown in Fig. 7. Further, as the result of their mathematical product increases, the output power also increases. Therefore, the conventional TE module with Π-type elements ($\theta = 90°$) is the most appropriate for our assumptions.

The distribution of current density inside the TE module is precisely examined as a function of the tilting angle of the elements, as shown in Fig. 8. At smaller tilting angles such as $\theta = 20°$ and 30°, a higher current density is homogenously

distributed in nearly the whole TE element. At areas close to the two terminals of the longer diagonal, a lower density is expected. This irregular distribution disappears gradually with an increase in θ. The higher and lower density regions share the element almost equally at $\theta = 80°$. Thus, a clear boundary between the higher and lower density regions cannot be determined, and all the charges move homogenously inside the entire TE elements at $\theta = 90°$, as an extreme case. This phenomenon is illustrated in Fig. 9.

A 3-d mainstream domain is taken as an example at a tilting angle $\theta = 60°$ and illustrated in Fig. 9(a). This domain is sandwiched between two parallel surfaces A-1 and A-2 and is enclosed by two intersectional surfaces B-1 and B-2. This mainstream domain is widened at larger tilting angles, for example, at $\theta = 80°$ shown in Fig. 9(b)-1. The length of the sidestream region is shortened so that more electric charges choose to flow in this domain when compared with the case shown in Fig. 9(a), and the charge-transporting ability of the stream is enhanced. In this case, the difference in the lengths of the main- and sidestreams is reduced, and the electric current is more evenly allocated to them. The distribution of current density becomes more homogenous with the combination of the two streams having similar charge-transporting abilities. This scheme is reflected in the contours of current density shown in Fig. 9(b)-2. In the extreme case of a tilting angle $\theta = 90°$, the mainstream domain covers the entire element, and the sidestream is further shortened to the same length as that of the mainstream, as shown in Fig. 9(c)-1. A homogenous distribution of current density is produced by the coactions of the two streams having nearly same charge-transporting abilities, as shown in Fig. 9(c)-2.

The two borders A-1 and A-2 of the mainstream domain gradually move closer with a decrease in the tilting angle until they overlap at $\theta = 45°$. Then, the mainstream domain becomes a plane, as shown in Fig. 9(d). Further, the mainstream domain disappears at smaller tilting angles ($\theta < 45°$) and is replaced by a new domain in the shape of a parallelogram. This domain can be considered as a rectangular area, whose triangular corners (C-1 and C-2) are removed, as shown in Fig. 9(e). The smaller tilting angle makes the TE elements narrower so that the main- and sidestreams are closer because of the space restriction. Therefore, the difference in the lengths of these two streams becomes smaller again. These two reasons contribute to the homogenous distribution of the current density in the entire elements, as another extreme case shown in Fig. 9(f).

The curve of the output power in Fig. 7 might be considered to consist of two parts: concave and convex. They are separated at a certain tilting angle (angle boundary indicated by a dashed line), as shown in Fig. 10. If the concave part continues to maintain its course, and if the convex part is replaced by an imaginary curve, it is probably feasible to enhance the performance of the TE module using elements having a small tilting angle. Finally, on the basis of the results of this study, we may propose a novel geometry, as illustrated in the subgraph of Fig. 10, wherein the low-density regions are removed and the element body is widened to save thermal energy and materials and depress the resistance of the TE module. The effectiveness of this design will be reported separately.

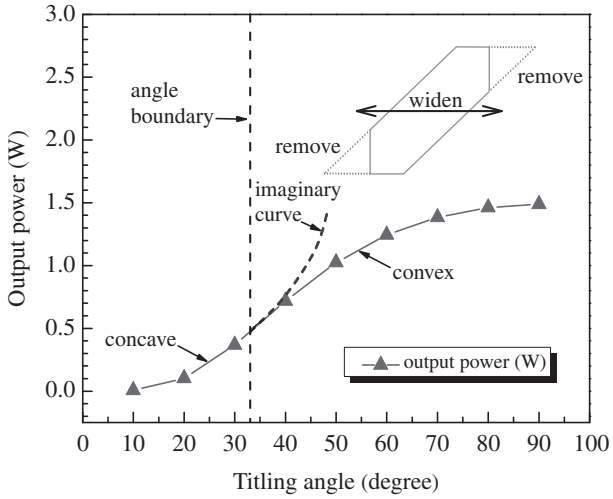

Fig. 10 A new shape concept of TE element for higher performance.

4. Conclusions

In this paper, a thermoelectric module is designed by using tilted elements, which are electrically connected in series. The performance of these TE elements is numerically analyzed, and the tilting angle is shown to have a significant impact on the performance because of the change of the internal electric resistance. Further, the TE performance increased until the tilting angle approached 90°. Therefore, the conventional TE module with Π-type elements ($\theta = 90°$) is considered to be the most favorable. Moreover, the TE performance of the two modules consisting of elements arranged in parallel and symmetrical configurations with tilting angles 45 and 135°, respectively, is not significantly affected.

The module configuration and element shape determine the distribution of temperature and current density inside the TE module. The mainstream of the current is chosen preferentially from the geometry of the TE element, and the shortest path is selected. Most of electric charge flows along the mainstream, and the rest of the charge moves along the sidestream. A homogenous high-density region is formed at the center of the element when these streams overlap. The charge-transporting ability is influenced by the length of the main- and sidestreams.

Acknowledgements

The authors are especially grateful for the financial supports from the JST-CREST, Research Grant-in-Aid of JSPS (No. 2402077), and JSPS Fellowship.

REFERENCES

1) T. Aoki, C. Wan, H. Ishiguro, H. Morimitsu and K. Koumoto: J. Ceram. Soc. Jpn. **119** (2011) 382–385.
2) T. Sakamoto, T. Iida, A. Matsumoto, Y. Honda, T. Nemoto, J. Sato, T. Nakajima, H. Taguchi and Y. Takanashi: J. Electron. Mater. **39** (2010) 1708–1713.
3) A. J. Zhou, T. J. Zhu, X. B. Zhao, S. H. Yang, T. Dasgupta, C. Stiewe, R. Hassdorf and E. Mueller: J. Electron. Mater. **39** (2010) 2002–2007.
4) K. Koumoto, R. Funahashi, E. Guilmeau, Y. Miyazaki, A. Weidenkaff, Y. Wang and C. Wan: J. Am. Ceram. Soc. **96** (2013) 1–23.

5) R. O. Suzuki, Y. Sasaki, T. Fujisaka and M. Chen: J. Electron. Mater. **41** (2012) 1766–1770.
6) S. B. Riffat and G. Q. Qiu: Int. J. Energy Res. **30** (2006) 67–80.
7) R. O. Suzuki: J. Power Sources **133** (2004) 277–285.
8) A. Z. Sahin and B. S. Yilbas: Energy Conv. Manag. **65** (2013) 26–32.
9) A. Takezawa and M. Kitamura: Int. J. Numer. Methods Eng. **90** (2012) 1363–1392.
10) R. O. Suzuki and D. Tanaka: J. Power Sources **122** (2003) 201–209.
11) X. Meng, T. Fujisaka and R. O. Suzuki: J. Electron. Mater. **43** (2014) 1509–1520.
12) K. Takahashi, T. Kanno, A. Sakai, H. Tamaki, H. Kusada and Y. Yamada: Sci. Rep. **3** (2013) 1501.
13) T. Kanno, A. Sakai, K. Takahashi, A. Omote, H. Adachi and Y. Yamada: Appl. Phys. Lett. **101** (2012) 011906.
14) D. M. Rowe: *CRC Handbook of Thermoelectrics*, (CRC Press, Florida, 1995) pp. 445–446.
15) T. Fujisaka, H. Sui and R. O. Suzuki: J. Electron. Mater. **42** (2013) 1688–1696.